

Preferred functionalization of metallic and small-diameter single walled carbon nanotubes *via* reductive alkylation†

D. Wunderlich, F. Hauke and A. Hirsch*

Received 30th October 2007, Accepted 6th December 2007

First published as an Advance Article on the web 4th January 2008

DOI: 10.1039/b716732f

A selectivity investigation of the covalent sidewall functionalization of SWNTs by reductive alkylation (Billups reaction) is reported. The functionalized tubes R_n -SWNT were characterized by UV-vis-NIR absorption, nIR emission and Raman spectroscopy. The reduction of SWNTs with sodium and the subsequent alkylation of the reduced tubes $SWNT^{n-}$ with butyl iodide reveal a pronounced SWCNT diameter dependence, that is, SWNTs with smaller diameter are considerably more reactive than tubes with larger diameter. Moreover, this reaction sequence also favours the preferred functionalization of metallic over semiconducting tubes. Treatment of the reduced intermediates $SWNT^{n-}$ with protons, *via* the use of ethanol, instead of alkyl iodide leads to hydrogenated tubes. However, in this case the degree of functionalization is considerably lower than that observed for the corresponding alkylation. Also no pronounced preference of the reaction of metallic and small diameter tubes was observed during the hydrogenation process.

Introduction

For the application of carbon nanotubes¹ in electronic devices one major challenge has still to be overcome, namely the efficient separation of metallic and semiconducting species. One conceptual approach to address this problem is to take advantage of the different chemical reactivities of metallic and semiconducting tubes with respect to sidewall functionalization. First experimental evidence for preferred reactions of metallic *versus* semiconducting tubes towards addition reactions has been provided for some reactions^{2–4} such as diazonium functionalization or nucleophilic alkylation followed by oxidation. These preferences can be explained by the availability of electronic states close to the Fermi level, which in the case of the reaction with nucleophiles are unoccupied states (Fig. 1).⁴ Along the same lines this selectivity can also be explained by a traditional chemistry concept, reported by Joselevich, stating that the metallic species are less aromatic and have a smaller HOMO–LUMO gap.⁵ We have recently shown in a detailed investigation that this holds for a whole variety of nucleophilic additions to the sidewalls of SWNTs including those of Grignard compounds.⁶ Simultaneously, we could also prove that the addition reaction of organometallic compounds is diameter dependent, namely, that *the reactivity is inversely proportional to the SWNT diameter*. This diameter dependent selectivity of addition reactions is expected,^{7,8} but except for the addition of diazonium salts² no detailed experimental investigation has been reported before.

So far, for two other important SWNT sidewall functionalization reactions, which are the hydrogenation of carbon nanotubes by reduction with sodium and treatment with ethanol described

by Pekker *et al.*⁹ and the reductive alkylation reported by Billups *et al.*¹⁰ (Scheme 1), investigations concerning their selectivity with respect to a specific tube type have not been carried out. We now report a selectivity study for these reactions using the same spectroscopic criteria that we have published recently for the selective reaction of tubes with organometallic compounds.⁶ We demonstrate that i) the reduction of SWNTs with sodium and the subsequent alkylation exhibits a pronounced SWNT diameter dependence: the reactivity of SWNTs is inversely proportional to the diameter for both metallic and semiconducting SWNTs, ii) compared to alkylation, protonation of the negatively charged intermediates $SWNT^{n-}$ leads to considerable lower degrees of functionalization, iii) no pronounced diameter selectivity can be detected for the hydrogenation reaction, iv) the hydrogenation shows no distinct selectivity to either metallic or semiconducting tubes, v) the reduction of SWNTs with sodium and the subsequent alkylation exhibits a pronounced selectivity to metallic tubes and vi) the functionalized semiconducting tubes still fluoresce in the near infrared (nIR).

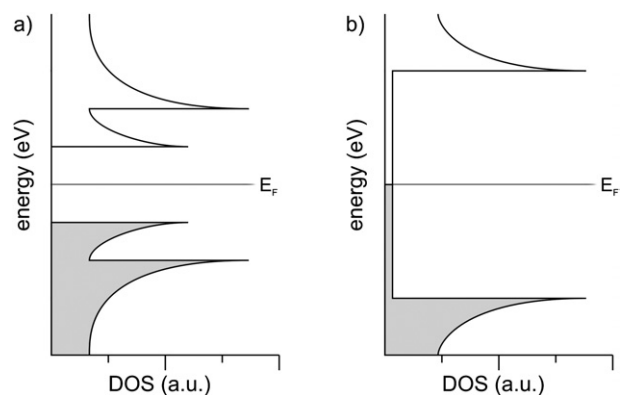
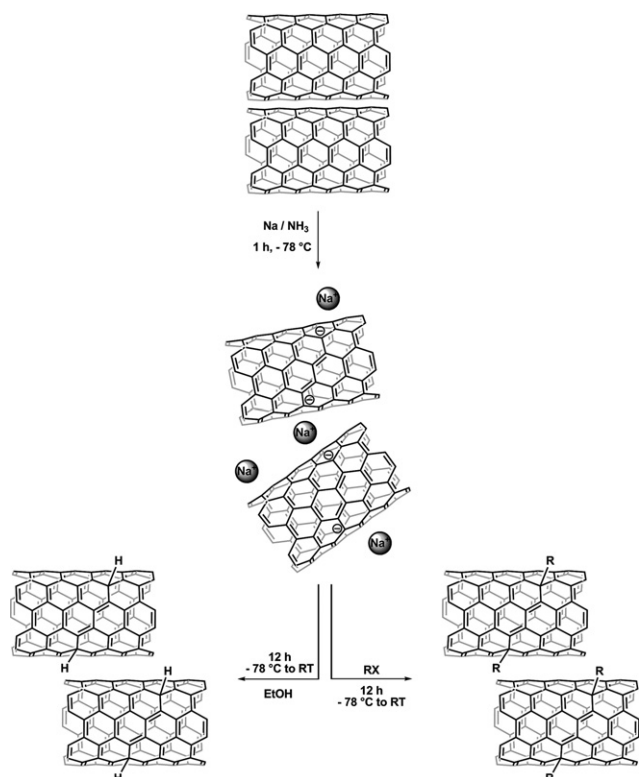


Fig. 1 Schematic representation of the density of electronic states (DOS) for a semiconducting (left) and a metallic nanotube (right).

Department of Chemistry and Pharmacy & Central Institute of Advanced Materials and Processes (ZMP) University of Erlangen-Nürnberg, Erlangen, 91054, Germany. E-mail: hirsch@chemie.uni-erlangen.de; Fax: (+49) 9131-8526864

† This paper is part of a *Journal of Materials Chemistry* theme issue on carbon nanostructures.



Scheme 1 Reductive hydrogenation and alkylation of SWNTs in liquid ammonia by sodium and ethanol or an alkyl halide (RX).

Experimental

Materials and instrumentation

SWNTs (batch number P0335) were obtained from Carbon Nanotechnologies Inc. (Super Purified HiPco® Single-Wall Carbon Nanotubes) and used as received. Chemicals and solvents were purchased from Acros (Geel, Belgium) and also used as received. Ammonia (99.9990 vol.% purity) was purchased from Riessner Gase. Raman spectra of each sample were recorded from the solid (bucky-paper) at three different points and averaged with a Thermo Nicolet Almega XR Dispersive Raman Spectrometer ($\lambda_{\text{ex}} = 532 \text{ nm}$ and 780 nm). The spectra showing the D- and G-bands are normalized to the G-band, the spectra showing the radial breathing modes (RBMs) are normalized to the (9,3)-mode (532 nm excitation) and the (10,2)-mode (780 nm excitation). Samples for fluorescence and UV-vis-nIR measurements were prepared in a one percentage solution of sodium dodecylbenzenesulfonate (SDBS) in deuterated water (0.25 mg SWNTs per mL). The spectra were measured from the supernatant after sonication (5 min) and precipitation (1 d) of the insoluble SWNTs. Sonications were performed with a Bandelin Sonorex RK 106 or with a Hielscher UP400S Ultrasonic Processor. Fluorescence spectra were recorded with a NS1 NanoSpectra-lyzer ($\lambda_{\text{ex}} = 660 \text{ nm}$ and 785 nm) from Applied NanoFluorescence, LLC. The spectra were normalized to the minimum at 1160 nm (660 nm excitation) and 1140 nm (785 nm excitation). UV-vis-nIR spectra were recorded with a Shimadzu UV3102-PC instrument and normalized to the minimum at 628 nm .

General procedure for the synthesis of R_n -SWNT

In a nitrogen-purged, heat dried and cooled ($-78 \text{ }^\circ\text{C}$, acetone/dry-ice) four-necked round bottom flask (250 mL), equipped with two gas inlets, pressure compensation and a mechanical stirrer, ammonia (100 mL) was condensed. The HiPco SWNTs (30 mg, 2.5 mmol of carbon) and sodium (23 mg, 1.0 mmol) were added in small portions and stirred for one hour, yielding a stable, blue-black, homogeneous dispersion. To this dispersion 1-iodobutane (0.12 mL, 1.0 mmol) (for the preparation of Bu_n -SWNT) was added dropwise over a period of 10 min. For the preparation of H_n -SWNT no further reagent was added to the dispersion of charged nanotubes. Subsequently the cooling bath was removed and the ammonia was evaporated off overnight under a small flow of nitrogen gas. By-products such as salts and unreacted sodium were removed by dissolution of the solid reaction mixture in ethanol (100 mL) under sonication (15 min). Subsequently, the resulting heterogeneous dispersion was diluted with water (100 mL), acidified with hydrochloric acid (1 mL, 37%) and transferred into a separation funnel with cyclohexane (100 mL). The water/ethanol phase was discarded and the cyclohexane layer with the functionalized nanotubes was repeatedly purged with water until the pH value remained neutral. The organic layer with the nanotubes was filtered through a PP membrane filter ($0.2 \mu\text{m}$) and washed with ethanol, methanol and water. The resulting black solid was dried in a vacuum oven ($50 \text{ }^\circ\text{C}$) overnight yielding a bucky-paper of R_n -SWNT. For the preparation of H_n -SWNT, the intermediate nanotube salt Na_n -SWNT (see above) was treated with ethanol (100 mL) under sonication (15 min). The rest of the work up was carried out as described for the Bu_n -SWNT samples.

Results and discussion

The primary characterization tool for the structural investigation of sidewall functionalized SWNTs is Raman spectroscopy.¹¹ The covalent addition to and therefore re-hybridization of sidewall C atoms significantly influences the intensity ratio of the SWNT Raman bands.^{12,13} The most noticeable change consists of an increase in intensity of the D-band ($\sim 1250\text{--}1450 \text{ cm}^{-1}$), which arises from the generation of $\text{sp}^3\text{-C}$ atoms as defects in the sidewalls, relative to those of the radial breathing modes (RBMs) ($\sim 100\text{--}300 \text{ cm}^{-1}$) and the G-band ($\sim 1500\text{--}1600 \text{ cm}^{-1}$). The intensity ratio between the D-band and the G-band ($A_{\text{D}}/A_{\text{G}}$) is therefore taken as a parameter for the extent of functionalization.^{12,13}

In the present study all Raman spectra are normalized to the G-band intensity. As Raman spectroscopy is a resonant process, it is possible to address different kinds of SWNTs with different excitation wavelengths. The assignment of tubes that are resonant for a given wavelength was a subject of careful systematic investigations and can be taken from the so-called Kataura plots.^{3b,14} For our investigations two different excitation wavelengths (532 and 780 nm) were used. Excitation at 532 nm is predominantly resonant for metallic nanotubes, whereas the excitation wavelength of 780 nm leads to a predominant excitation of semi-conducting tubes.^{3b}

For the Raman measurements R_n -SWNT samples prepared as bucky-papers were used. The G-bands obtained with the

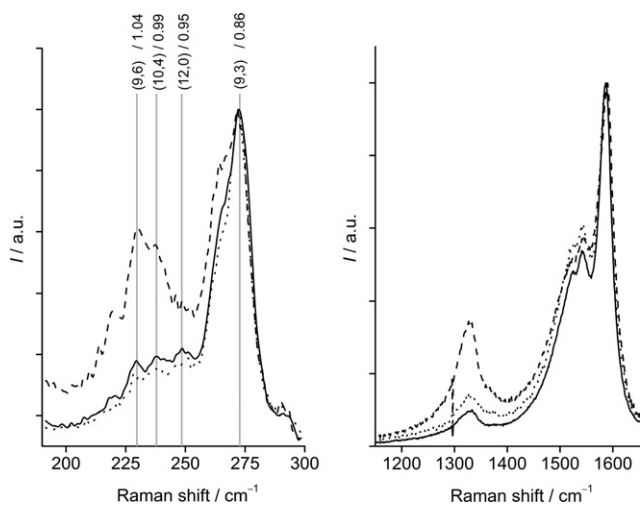


Fig. 2 Raman spectra (532 nm excitation) of pristine SWNT (black line), H_n -SWNT (dotted line) and Bu_n -SWNT (dashed line) with chiral indices and diameters in nm— $(n,m)/d$.

excitation wavelength of 532 nm exhibit a pronounced asymmetry at the low frequency side, which is attributed to a Breit–Wigner–Fano (BWF) resonance of metallic nanotubes (Fig. 2, right). At the excitation wavelength of 780 nm the G-band splits into a higher (G^+) and a lower (G^-) frequency component, both exhibiting a symmetric line shape and being attributed to semiconducting nanotubes (Fig. 3, right).¹⁵

With HiPco nanotubes four easily distinguishable, predominant metallic M_{11} transitions at 229 cm^{-1} , 239 cm^{-1} , 248 cm^{-1} and 273 cm^{-1} can be detected (Fig. 2, left). Based on the equation $\omega_{\text{RBM}} = Ad_t^{-1} + B$ ($A = 223.5 \text{ nm cm}^{-1}$ and $B = 12.5 \text{ cm}^{-1}$)¹⁶ the diameters of the corresponding tubes can be calculated: (from left to right) 1.04, 0.99, 0.95 and 0.86 nm. Therefore it is possible to assign the peaks to the (9,6), (10,4), (12,0) and (9,3) chirality indices by the use of a modified Kataura plot.^{3b} As mentioned before, all RBM regions with 532 nm excitation wavelengths are normalized to the (9,3)-mode.

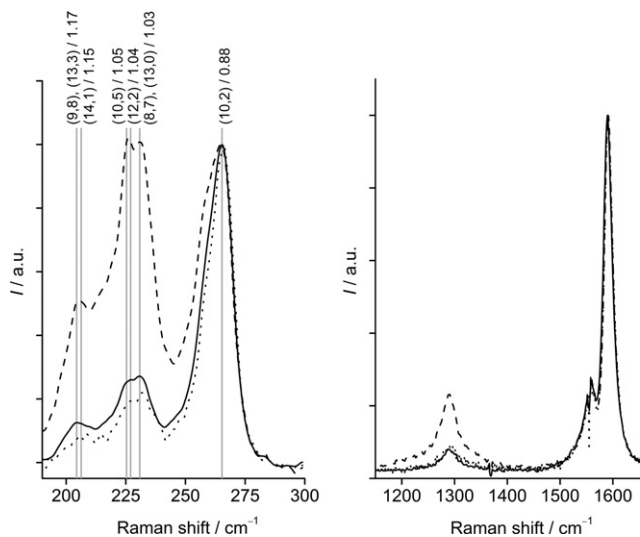


Fig. 3 Raman spectra (780 nm excitation) of pristine SWNT (black line), H_n -SWNT (dotted line) and Bu_n -SWNT (dashed line) with chiral indices and diameters in nm— $(n,m)/d$.

Table 1 Comparison of the Raman (A_D/A_G) ratios of H_n -SWNTs and Bu_n -SWNTs

Sample	Raman 532nm ^a	Raman 780nm ^a
H_n -SWNT	1.4	1.7
Bu_n -SWNT	5.3	3.8

^a Values are the ratios A_D/A_G relative to A_{D0}/A_{G0} of the pristine SWNTs excited at the denoted wavelength.

At 780 nm excitation four distinguishable S_{22} bands for semiconducting tubes at 205 cm^{-1} , 226 cm^{-1} , 230 cm^{-1} and 265 cm^{-1} can be identified (Fig. 3, left). Using the Kataura plot these can be attributed to eight different chirality indices: 204 cm^{-1} (9,8) and/or (13,3), 206 cm^{-1} (14,1), 225 cm^{-1} (10,5), 227 cm^{-1} (12,2), 230 cm^{-1} (8,7) and/or (13,0) and 265 cm^{-1} (10,2), respectively. The corresponding diameters are 1.17, 1.15, 1.05, 1.04, 1.03 and 0.88 nm. Spectra with 780 nm excitation showing the RBM region are normalized to the (10,2) mode. The values for the A_D/A_G ratio relating to A_{D0}/A_{G0} of the pristine SWNTs are listed in Table 1.

Addition of ethanol to the reduced SWNTⁿ⁻ leads to sidewall hydrogenation (Scheme 1, left). However, as can be clearly seen from the Raman spectra (Fig. 2 and 3) no pronounced increase of intensity of the D-bands is visible. In the RBM regime no significant changes are observable. This is in contrast to the spectra of the butylated derivatives Bu_n -SWNT which are depicted in dashed lines. The addition of alkylating reagents to the sodium reduced SWNTⁿ⁻ intermediates results in the formation of covalently functionalized SWNTs (Scheme 1, right). Apparently, 1-iodobutane is much more reactive towards reduced SWNTs than ethanol. If the protonation of SWNTⁿ⁻ is incomplete, leading to H_m -SWNT^{(n-m)-} ($n > m$) only, subsequent handling of a sample at ambient conditions is expected to oxidize H_m -SWNT^{(n-m)-} to H_m -SWNT with a lower degree of hydrogenation than theoretically possible.⁴ These more pronounced D-band intensity changes caused by the reductive alkylation correlate well with the changes in the RBM region. This leads to the conclusion that the protonation of the negatively charged tube intermediates results in a lower degree of functionalization compared with the reaction with primary aliphatic halides. In addition, the hydrogenation shows no pronounced selectivity at all.

However, a clear diameter dependence associated with the formation of Bu_n -SWNT can be deduced from the Raman results in the RBM regions. As mentioned before, the spectra have been normalized to the (9,3)-mode and (10,2)-mode, respectively. Excitation at both 532 and 780 nm reveals pronounced augmentation of signal intensities of the tubes with diameters larger than 0.86 nm and 0.88 nm, respectively. As the spectra have been normalized this can be translated into an intensity reduction for the peaks correlated with the (9,3)-tube in the metallic and the (10,2)-tube in the semiconducting regime. The decrease in RBM intensity in functionalized R_n -SWNT is due to reduction of symmetry caused by the binding of addends. Conceptually, an ensemble of functionalized tubes with a given (n,m) -helicity is expected to be completely desymmetrized, since even for the ideal case that every tube contains the same number of addends R, a myriad of regioisomers will be formed. The

conclusion from these results is that there is a pronounced diameter dependence in the case of the reductive alkylation: *the reactivity of the tubes correlates inversely with the diameter.*

Translated into a mechanical picture the following conclusion can be drawn. After the electron transfer of solubilized electrons to the SWNTs, the charged carbon nanotube intermediates SWNT⁻ are exfoliated due to the electrostatic repulsion and are therefore homogeneously dissolved as individual species in the liquid ammonia. Electrons are preferably located at smaller diameter nanotubes, having the highest degree of pyramidalization of the carbon framework. In analogy to the reduction of fullerenes and their derivatives, a high degree of pyramidalization leads to an efficient stabilization of negative charge.¹⁷ As in the case of the reaction of SWNTs with organometallic reagents followed by oxidation, the preferred functionalization of metallic tubes can be explained by the accessibility of density of states just above the Fermi level, leading to a more facile reduction of metallic tubes.^{4,6} The not-pronounced diameter selectivity of the hydrogenation can presumably be explained by the heterogeneous functionalization sequence. The protonation of the charged nanotube material by ethanol takes place in the solid state. Here, in contrast to the individualized tubes in solution, one has to deal with bulk effects, which lead to a uniform functionalization of all present tube species. This could also explain why the hydrogenation reaction sequence does not lead to a pronounced selectivity regarding metallic and semiconducting species.

As we have shown earlier, nIR fluorescence spectroscopy can also be used as another very powerful and very sensitive tool for the specific characterization of SWNT derivatives.⁶ The near-infrared photoluminescence across the band gap in semiconducting tubes can only be detected in isolated SWNTs. An interaction with neighboring metallic nanotubes in SWNT bundles would quench the fluorescence.¹⁸ The individualization of the functionalized material was accomplished by the use of SDBS as a surfactant in deuterated water.¹⁹ All functionalized samples exhibit lower fluorescence intensities than the starting material. To assign the observed S₁₁ bands to nanotube chirality indices and diameters, we used a Kataura plot,²⁰ based on empirical results of spectrofluorimetric data for identified SWNTs in aqueous SDS suspension and fitted to empirical expressions. Fig. 4 shows the typical fluorescence spectra of the pristine HiPco material (black line) at 660 and 785 nm excitation wavelengths.

The bands at 952, 976, 1024, 1061, 1111, 1124, 1179, 1208, 1249, 1259, 1276, 1328 and 1379 nm can be attributed from left to right to the indices (8,3), (6,5), (7,5), (8,4), (7,6), (8,6), (11,3), (9,5), (10,3) and/or (10,5), (8,7) and/or (11,1), (9,7) and (10,6) and/or (12,2) with the diameters of 0.78, 0.76, 0.83, 0.88, 0.84, 0.90, 0.97, 1.01, 0.98, 0.94 and/or 1.05, 1.03 and/or 0.92, 1.10, 1.11 and/or 1.04 nm.²⁰ The fluorescence spectra of H_n-SWNT are also depicted in Fig. 4. For better comparability the spectra were normalized to the minimum at 1160 nm (660 nm excitation) and 1140 nm (785 nm excitation), respectively. The results are in good agreement with the Raman investigation, as no pronounced diameter dependence can be deduced. This is again in significant contrast to the spectra of the butylated SWNT derivatives (Bu_n-SWNT). Here, the tubes with small diameters attributed to chirality indices (8,3) up to (7,6) have partly or almost completely disappeared or at least strongly decreased, in contrast to the larger diameter tubes (indices (8,6) up to (10,6)).

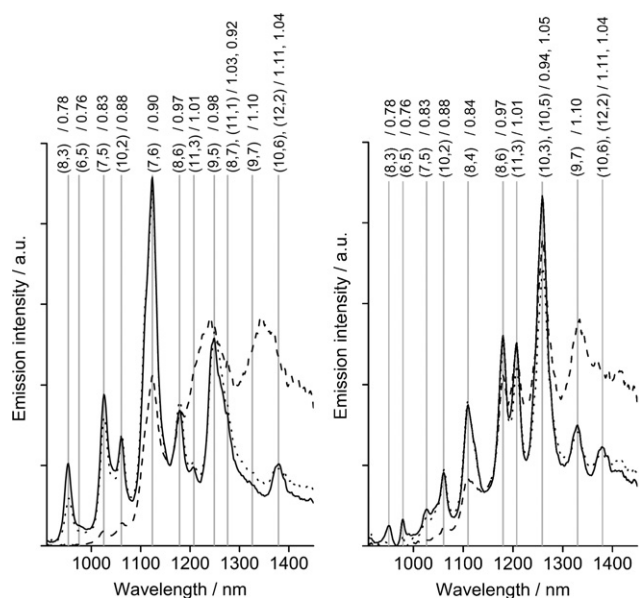


Fig. 4 Fluorescence spectra (left: 660 nm excitation, right: 785 nm excitation) of pristine SWNTs (black line), H_n-SWNT (dotted line) and Bu_n-SWNT (dashed line) with chirality indices and diameters in nm—(n,m)/d.

The disadvantage of the very sensitive nIR fluorescence spectroscopy is that it can sense only semiconducting carbon nanotubes. In contrast, UV-vis-nIR absorption spectroscopy highlights all tubes present in the sample. Fig. 5 depicts the spectra of the pristine material suspended in D₂O/SDBS and also in D₂O/DOC (sodium deoxycholate) after centrifugation (25 000 g). By this treatment the bundles are disintegrated and the supernatant consists of well dispersed and isolated tubes.

The peak intensities in the range between 400 to 645 nm, representing the first van Hove transitions of metallic species (M₁₁), overlap slightly with the second van Hove transitions of semiconducting species (S₂₂) in the 550 to 900 nm region. The first electronic transition of the semiconducting SWNT (S₁₁)

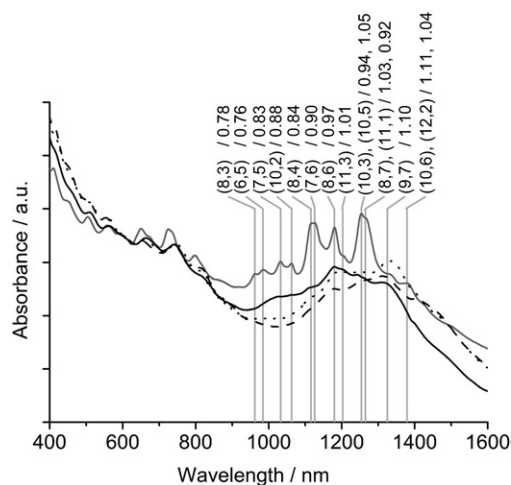


Fig. 5 UV-vis-nIR spectra of pristine SWNTs in D₂O/SDBS (black line) and D₂O/DOC (grey line), H_n-SWNT (dotted line) and Bu_n-SWNT (dashed line) (both in D₂O/SDBS) with chirality indices and diameters in nm—(n,m)/d.

can be detected in the region between 800 and 1600 nm. The spectrum of pristine tubes dispersed in D₂O/DOC affords the assignment of the peaks of the S₁₁ transitions to the corresponding chirality indices. Compared to the spectra used for the reported Kataura plot²⁰ we observe an average bathochromic peak shift of about 5.5 nm in the region between 962 and 1379 nm. The identified chirality indices and diameters depicted in Fig. 5 are as follows: 962 nm (8,3), 984 nm (6,5), 1033 nm (7,5), 1063 nm (10,2), 1111 nm (8,4), 1120 nm (7,6), 1180 nm (8,6), 1203 nm (11,3), 1254 nm (10,3)/(10,5), 1265 nm (8,7)/(11,1), 1325 nm (9,7) and 1379 nm (10,6)/(12,2). Hence, all chirality indices observed by fluorescence spectroscopy are also detectable by UV-vis-nIR spectroscopy with exception of the (9,5)-tubes. All UV-vis-nIR spectra are normalized to the absorbance minimum at 628 nm for better comparability. A close look at the S₁₁ region in the spectra of the H_n-SWNTs (dotted) and Bu_n-SWNTs (dashed) reveals confirmation of the results obtained by the nIR emission experiments. In the case of the alkylated derivatives Bu_n-SWNT the absorbance of functionalized tubes is strongly reduced in the domain of the smaller diameter tubes compared to the larger diameter counterparts.

Conclusion

We report here for the first time a selectivity investigation of the covalent sidewall functionalization of SWNTs by reductive alkylation (Billups reaction). In analogy to a related functionalization method that we reported earlier, namely the treatment of SWNTs with organometallic reagents followed by oxidation, we find that SWNTs with smaller diameter are considerably more reactive than tubes with larger diameter. Moreover, this reaction sequence favours also the preferred functionalization of metallic over semiconducting tubes. The corresponding hydrogenation sequence consisting of reduction of SWNTs with sodium and protonation of the intermediates SWNTⁿ⁻ in the solid state, however, shows no significant selectivity and also leads to a very low overall conversion. We explain this by the lower electrophilicity of ethanol acting as a proton source and by the facile air oxidation of charged or 'deprotonated' intermediates H_n-SWNT^{(n-m)-}. The preferred functionalization of metallic and small diameter tubes found for the Billups reaction bears promising potential for the separation of SWNTs according to diameter and metallic character taking into account that functionalized tubes show improved solubility properties. After fractioning of the functionalized tubes *via* extraction procedures the original electronic properties are expected to be recovered by thermal cleavage of the addends.

Acknowledgements

This work was supported by the Deutsche Forschungsgemeinschaft (DFG). We thank the Interdisciplinary Center for Molecular Materials (ICMM) for financial support.

References

1 (a) See for example: K. Tanaka, T. Yamabe and K. Fukui, *The Science and Technology of Carbon Nanotubes*, Elsevier, Oxford, 1999; (b) P. Avouris, G. Dresselhaus and M. S. Dresselhaus,

Carbon Nanotubes: Synthesis, Structure, Properties and Applications, Springer-Verlag, Berlin, 2000; (c) S. V. Rotkin and S. Subramoney, *Applied Physics of Carbon Nanotubes*, Springer-Verlag, Berlin, 2005.

2 N. Nair, W.-J. Kim, M. L. Usrey and M. S. Strano, *J. Am. Chem. Soc.*, 2007, **129**, 3946.

3 (a) M. S. Strano, C. A. Dyke, M. L. Usrey, P. W. Barone, M. J. Allen, H. Shan, C. Kittrell, R. H. Hauge, J. M. Tour and R. E. Smalley, *Science*, 2003, **301**, 1519; (b) M. S. Strano, *J. Am. Chem. Soc.*, 2003, **125**, 16148; (c) K. H. An, J. S. Park, C.-M. Yang, S. Y. Jeong, S. C. Lim, C. Kang, J.-H. Son, M. S. Jeong and Y. H. Lee, *J. Am. Chem. Soc.*, 2005, **127**, 5196; (d) S. Toyoda, Y. Yamaguchi, M. Hiwatshi, Y. Tomonari, H. Muratami and N. Nakashima, *Chem.-Asian J.*, 2007, **2**, 145.

4 R. Graupner, J. Abraham, D. Wunderlich, A. Vencelova, P. Lauffer, J. Röhl, M. Hundhausen, L. Ley and A. Hirsch, *J. Am. Chem. Soc.*, 2006, **128**, 6683.

5 E. Joselevich, *ChemPhysChem*, 2004, **5**, 619.

6 D. Wunderlich, F. Hauke and A. Hirsch, *Chem.-Eur. J.*, 2008, DOI: 10.1002/chem.200701038.

7 Z. Chen, W. Thiel and A. Hirsch, *ChemPhysChem*, 2003, **1**, 93.

8 (a) J. L. Bahr and J. M. Tour, *J. Mater. Chem.*, 2002, **12**, 1952; (b) X. Lu, F. Tian, X. Xu, N. Wang and Q. Zhang, *J. Am. Chem. Soc.*, 2003, **125**, 10459; (c) K. Seo, K. A. Park, C. Kim, S. Han, B. Kim and Y. H. Lee, *J. Am. Chem. Soc.*, 2005, **127**, 15724.

9 S. Pekker, J.-P. Salvetat, E. Jakab, J.-M. Bonard and L. Forró, *J. Phys. Chem. B*, 2001, **105**, 7938.

10 (a) F. Liang, A. K. Sadana, A. Peera, J. Chattopadhyay, Z. Gu, R. H. Hauge and W. E. Billups, *Nano Lett.*, 2004, **4**, 1257; (b) F. Liang, L. B. Alemany, J. M. Beach and W. E. Billups, *J. Am. Chem. Soc.*, 2005, **127**, 13941; (c) J. Chattopadhyay, A. K. Sadana, F. Liang, J. M. Beach, Y. Xiao and W. E. Billups, *Org. Lett.*, 2005, **7**, 4067.

11 (a) See for example: M. S. Dresselhaus, G. Dresselhaus, A. Jorio, A. G. Souza Filho, M. A. Pimenta and R. Saito, *Acc. Chem. Res.*, 2002, **35**, 1070; (b) M. S. Dresselhaus, G. Dresselhaus, R. Saito and A. Jorio, *Phys. Rep.*, 2005, **409**, 47.

12 (a) See for example: A. Hirsch, *Angew. Chem., Int. Ed.*, 2002, **41**, 1853; A. Hirsch, *Angew. Chem.*, 2002, **114**, 1933; (b) O. Vostrowsky and A. Hirsch, *Angew. Chem., Int. Ed.*, 2004, **43**, 2326; O. Vostrowsky and A. Hirsch, *Angew. Chem.*, 2004, **116**, 2380; (c) C. A. Dyke and J. M. Tour, *J. Phys. Chem. B*, 2004, **108**, 11151; (d) K. Balasubramanian and M. Burghard, *Small*, 2005, **1**, 180; (e) S. Banerjee, T. Hemraj-Benny and S. S. Wong, *Adv. Mater.*, 2005, **17**, 17; (f) A. Hirsch and O. Vostrowsky, *Top. Curr. Chem.*, 2005, **245**, 193; (g) D. Tasis, N. Tagmatarchis, A. Bianco and M. Prato, *Chem. Rev.*, 2006, **106**, 1105.

13 M. Burghard, *Surf. Sci. Rep.*, 2005, **58**, 1.

14 (a) H. Kataura, Y. Kumazawa, Y. Maniwa, I. Umezū, S. Suzuki, Y. Ohtsuka and Y. Achiba, *Synth. Mater.*, 1999, **103**, 2555; (b) M. Hulman, R. Pfeiffer and H. Kuzmany, *New J. Phys.*, 2004, **6**, 1; (c) H. Telg, J. Maultzsch, S. Reich, F. Hennrich and C. Thomsen, *Phys. Rev. Lett.*, 2004, **93**, 177401; (d) A. Jorio, C. Fantini, M. A. Pimenta, R. B. Capaz, G. G. Samsonidze, G. Dresselhaus, M. S. Dresselhaus, J. Jiang, N. Kobayashi and R. Saito, *Phys. Rev. B*, 2005, **71**, 075401.

15 A. Kukuvecz, T. Pichler, R. Pfeiffer, C. Kramberger and H. Kuzmany, *Phys. Chem. Chem. Phys.*, 2003, **5**, 582.

16 (a) S. M. Bachilo, M. S. Strano, C. Kittrell, R. H. Hauge, R. E. Smalley and R. B. Weisman, *Science*, 2002, **298**, 2361; (b) A. Kukuvecz, C. Kramberger, V. Georgakilas, M. Prato and H. Kuzmany, *Eur. Phys. J. B*, 2002, **28**, 223; (c) V. C. Moore, M. S. Strano, E. H. Haroz, R. H. Hauge, R. E. Smalley, J. Schmidt and Y. Talmon, *Nano Lett.*, 2003, **3**, 1379.

17 A. Hirsch and M. Brettreich, *Fullerenes: Chemistry and Reactions*, Wiley-VCH, Weinheim, 2005.

18 M. J. O'Connell, S. M. Bachilo, C. B. Huffman, V. C. Moore, M. S. Strano, E. H. Haroz, K. L. Rialon, P. J. Boul, W. H. Noon, C. Kittrell, J. Ma, R. H. Hauge, R. B. Weisman and R. E. Smalley, *Science*, 2002, **297**, 593.

19 (a) C. A. Dyke and J. M. Tour, *Nano Lett.*, 2003, **3**, 1215; (b) V. C. Moore, M. S. Strano, E. H. Haroz, R. H. Hauge, R. E. Smalley, J. Schmidt and Y. Talmon, *Nano Lett.*, 2003, **3**, 1379.

20 R. B. Weisman and S. M. Bachilo, *Nano Lett.*, 2003, **3**, 1235.